Journal of Applied Fluid Mechanics, Vol. 13, No. 3, pp. 909-921, 2020.
Available online at www.jafmonline.net, ISSN 1735-3572, EISSN 1735-3645.
DOI: 10.29252/jafm.13.03.30448

Michell's Thin Ship Theory in Optimisation of Warp-Chine on Pentamaran Configuration

W. Sulistyawati, Yanuar † and A. S. Pamitran

Department of Mechanical Engineering, Universitas Indonesia, Depok, Jawa Barat 16425, Indonesia

†Corresponding Author Email: *yanuar@eng.ui.ac.id*

(Received April 28, 2019; accepted October 19, 2019)

ABSTRACT

This study was conducted to optimise warp–chine pentamaran configurations in wave cancellations to a significant total resistance reduction for a wide range of speed. The optimisation of a pentamaran with a warp–chine hull form was performed by a computer program Godzilla based on Michell's theory and validated by the towing test. The distance parameters of the outrigger were evaluated to select the lowest resistance generated. Computational analysis depended on the Michell–based tool compared to a commercial Computational Fluid Dynamics (CFD). The comparison of the measurement test of the total resistance and Michell's calculation results of all configurations showed a suitable trend, especially at Fn ≥ 0.4. However, it was not satisfactory for CFD trend. The illustrated of far-field wave pattern by the Michell-based instrument also consistent with the wave spectrum that captured in the test. The results of the analysis and observations revealed that the test measurement for all configuration models in the same estimated error (uncertainty) range of the total resistance. This optimisation has confirmed the stagger at the range of 0.36L–0.42L where the front outriggers and the after outriggers not in line of clearance as in arrow formation significant in wave cancellation and resistance reduction.

Keywords: Pentamaran; Warp–chine; Michell's theory; Optimisation; Wave cancellation; Resistance reduction.

NOMENCLATURE

A (θ)	amplitude
A_j (θ)	amplitude for multi hull with j numbered of hull
B_{CT}	bias limit
C_F	friction coefficient
C_R	residual coefficient
Cv	viscous coefficient
Cw	wave coefficient
$dR_W/d\theta$	free wave spectrum
F (θ)	interference between the hulls
G (θ)	complex expression of F(θ)
K	confidence level
k0	basic wave number
k (θ)	wave number at angle θ
(k+1)	form factor
P_{CT}	precision limit
R_T	total resistance
Rw	wave resistance
S	wetted surface area
S_{Dev}	standard deviation
s	longitudinal distance (stagger)
U_{CT}	uncertainty of total resistance coefficient
V	ship speed
w	lateral distance (clearance)
y=±Y	(x, y) hull surface
z=Z (x, y)	wave elevation
θ	angle and a propagating wave
ρ	water density
σ	displacement
σ_j	fraction of the total displacement of multihull
ω	phase function
ς (x,y)	wave pattern of ship at angles θ to x-axis direction of ship motion

1. INTRODUCTION

Optimal Multihull is formed by appropriate hull form and proper configuration of the outrigger, which results in minimum resistance that is a substantial impact on the overall performance and

economy of the ship. Computer engineering with advanced numerical simulations of geometrical on modification and optimisation algorithms have used in recent years. This method has been examined to yield the optimal solution in a large number of design variables. A numerical approach by Computational Fluid Dynamics (CFD) widely practised in the optimisation of the ship design. Even so, this process requires a high processor computer and several hours of running the programs.

Multihull needs to be carefully designed to avoid excessive wave and interference resistance, which is the most significant component in the total resistance. Some researchers have optimised the hull form and the side hull position through an experiment and computation. Many previous studies relied on the classic, linear thin ship theory, which is known as thin ship theory of Michell (1898). Doctors and Day (1995, 2000) applied it in optimising hull form of a monohull and a catamaran as well as an unconstrained sub-cushion parameter. They also developed a rapid method for investigating the near and far-field wave of Multihull (Day & Doctors 2001). Tuck and Lazaukas (1996) used the parameterisation of the hull in their optimisation study as well. They took note that optimum hulls could change significantly according to speed and separation. Mostly their research (Tuck & Lazauskas 1998, 2001) in numerical resistance of Multihull and optimisation studies of the side hull configuration. Also, they founded an impressive reduction in wave resistance, hull spacing and forward speeds. Other researchers (Day *et al*. 2003; Peng 2001; Moraes *et al*. 2004; Yeung *et al*. 2004) agreed that Michell's integral worked well with the towing test. Furthermore, Aubault and Yeung (2012) re-examined Multihull optimisation of the total wave resistance and tried it in shallow water.

In general, previous researchers of the pentamaran (Peng 2001; Ikeda *et al*. 2005; Dudson *et al*. 2005; Begovic *et al*. 2004; Tarafder *et al*. 2013; Yanuar *et al*. 2017) used slender ship models, such as the Wigley hull form. In this work is using warp-chine hull on pentamaran by investigating the resistance characteristics using a computer program "Michlet" (Lazaukas, 1997), which based on Michell's thin ship theory. The first studying is to specify the constraint interval on clearance and stagger (Sulistyawati *et al*. 2019 a, b). The primary objective of this advanced study is to obtain an optimum pentamaran configuration. The optimisation is using a computer program "Godzilla" (Lazauskas, 1997) that also based on Michell's thin ship theory. Those programs have proven and often accurate in wave estimator, determining ship resistance and consuming less time in the optimisation process of configuring Multihull and the shape of their hulls. The optimisation of a pentamaran with warp–chine hull form was performed by evaluating the distance parameters of the outrigger to select the lowest resistance generated. The shape optimisation of each hull was not in discussing. Furthermore, the results of those programs were in comparing with commercial CFD Ansys. At the end of this study, experiments in the towing tank on various configurations were performed to validate the numerical calculation.

2. MICHELL'S THIN SHIP THEORY

The application of Michell's thin ship theory (1898) analytically assumes the ship to be thin. Several studies have evidenced that this theory yielded relevant results with experimental variations in a higher Froude number (Fn), especially more than 0.4. In this work, the approach also provided a match with measurement of the towing test at Fn ≥ 0.4. However, at low Fn, it indicated a significant deviation.

2.1 Resistance

In Michell's theory, the ship is presenting a central plane source distribution in a steady wave pattern, $z=\zeta(x, y)$, which is active at various θ propagations relative to the negative x-axis direction of the ship's movement.

$$\varsigma(x, y) = R_W \int_{-\pi/2}^{\pi/2} A(\theta) e^{-ik(\theta)\omega(x,y,\theta)} d\theta \quad (1)$$

The complex amplitude function $A(\theta)$ related to the wave elevation of a ship expressed as the free wave spectrum or Kochin function (Tuck & Lazauskas, 1998); the wave number $k(\theta) = k_0 \sec^2\theta$; $k_0 = g/V^2$. V is the ship speed, g is gravity and a function of phase ω as $\omega = (x, y \text{ and } \theta) = x \cos\theta + y \sin\theta$, then Eq. (1) becomes:

$$\varsigma(x, y) = R_W \int_{-\pi/2}^{\pi/2} A(\theta) e^{-ik(\theta)\left[x\cos\theta + y\sin\theta\right]} d\theta \quad (2)$$

The wave amplitude function $A(\theta)$ is determined by the speed, and the form factor of the hull, that is expressed as Eq. (3). And Eq. (4) evaluates the hull surface, $Y(x, y)$, with a transom stern, in which the offset transom is indicated by $Y(xs, z)$:

$$A(\theta) = -\frac{2i}{\pi} k_0^2 \sec^4\theta \iint Y(x,z) e^{k_0 z \sec^2\theta + ik_0 x \sec\theta} dxdz \quad (3)$$

$$A(\theta) = -\frac{2i}{\pi} (k_0 \sec^2\theta)^2 \int_{-\infty}^{0}\int_{-\infty}^{\infty} Y(x,z) e^{ik_0 x\sec\theta} e^{ik_0 z\sec\theta} dxdz + \frac{2}{\pi}(k_0 \sec^3\theta) \int_{-\infty}^{0} Y(x_S, z) e^{k_0 z\sec^2\theta} dxdz \quad (4)$$

Newman (1977) argued that the energy left behind in the wave system is interrelated to the complex wave amplitude function $A(\theta)$ and to the wave resistance R_W, which is:

$$R_W = \frac{2}{\pi} \rho V^2 k_0^4 \int_{-\pi/2}^{\pi/2} \sec^5\theta d\theta \left| \iint_w Y(x,z) e^{ik_0 x\sec\theta + k_0 z\sec^2\theta} dxdz \right|^2 \quad (5)$$

$$R_W = \frac{\pi}{2}\rho V^2 \int_{-\pi/2}^{\pi/2} |A(\theta)|^2 \cos^3\theta d\theta \quad (6)$$

Where $Y(x, z)$ is the data off set of ships with x from bow to stern, y to starboard, and z upward from the free surface; W is the centre plane of the ship; ρ is the water density. The integral in the bar of Eq. (5), a complex amplitude function $A(\theta)$. Then the Michell integral for the wave resistance R_W can be written as Eq. (6).

In the Michell-based tool, offsets data was inputted to define the ship's hull, $y=\pm Y(x, y)$, which was represented in a grid point (x, y) and described as a body with waterlines and section. In conditions of convergence to verify the resistance, repetitions of waterline numbers and model sections varying from 33 to 81 (as maximum odd integers).

2.2 Multihull

According to Tuck and Lazauskas (1998) and Day *et al.* (2003), the wave resistance of Multihull is calculated by separating the waves of each hull into a single hull. Thence, the waves generated by amplitude functions are also considered single. Multihull with N numbered j hull is located at (x, y) = (x_j, y_j), produces wave amplitude $A_j(\theta)$:

$$A(\theta)=\sum_{j=1}^{N} e^{-ik(\theta)\sec^2\theta[x_j\cos\theta+y_j\sin\theta]}$$

$$\iint_{wj} Y_j(x,z)e^{ik_0[x\sec+z\sec^2\theta]}dxdz \quad (7)$$

where w_j is the centre plane to the centre point located at $(x, y) = (x_j, y_j)$. The wave amplitude function $A(\theta)$ of the entire hull is expressed as:

$$A(\theta) = \sum_{j=1}^{N} A_j(\theta)e^{ik(\theta)[x_j\cos\theta+y_j\sin\theta]} \quad (8)$$

The total far-field wave ζ is:

$$\varsigma(x, y) = \sum_{j=1}^{N} Rw\int_{-\pi/2}^{\pi/2} A_j$$

$$e^{[(x-xj)\cos\theta+(z-zj)\sin\theta]}d\theta \quad (9)$$

$A_j(\theta)$ is represented by

$$A_j(\theta) = \sigma_j A_0(\theta) \quad (10)$$

where σ_j is a fraction of the total displacement of Multihull. Then the combined wave amplitude $A(\theta)$ is:

$$A(\theta) = A_0(\theta)F(\theta) \quad (11)$$

$F(\theta)$ is the hull interference function—a factor of the wave-making of each hull expressed as:

$$F(\theta)=\int_{j=1}^{N}\sigma_j e^{ik(\theta)[xj\cos\theta+yj\sin\theta]} \quad (12)$$

which is a function of the arrangement pattern (x_j,y_j) and σ_j. By minimising $|F(\theta)|^2$, the optimisation can be possible (Tuck & Lazauskas, 1998).

2.3 Optimisation

Minimisation of total resistance Multihull is highly dependent on individual outrigger displacement, σ, stagger, s, and clearance, w, as well as by minimising the complex expression in Eq. (12). Hence, reducing the total resistance of Multihull by decreasing the magnitude of the complex interference of $G(\theta)$:

$$G(\theta) = |F(\theta)|^2 \quad (13)$$

The pentamaran with N = 5 consists of a centreline hull and four identical outriggers, two sides-by-two sides of the main hull. Their centre planes separated by a lateral distance of 4w and a longitudinal distance of 4s. Based on the mathematical formula from Tuck and Lazauskas (1998), we assume that the main hull displacement is σ_1=1-4σ, and outrigger hull's displacement is $\sigma_2 = \sigma_3 = \sigma_4 = \sigma_5 = \sigma$. The general expression of the complex interference factor $F(\theta)$ is:

$$F(\theta) = 1-\sigma_2-\sigma_3-\sigma_4-\sigma_5+\sigma_2 e^{ik(\theta)(-x_2\cos\theta+y_2\sin\theta)} + \sigma_3 e^{ik(\theta)(-x_3\cos\theta-y_3\sin\theta)} + \sigma_4 e^{ik(\theta)(x_4\cos\theta+y_4\sin\theta)} + \sigma_5 e^{ik(\theta)(x_5\cos\theta-y_5\sin\theta)} \quad (14)$$

The main hull is placed at the origin $x_1=y_1=0$, (x_2, y_2) = (-s, + w), (x_3, y_3) = (-s, -w), (x_4, y_4) = (s, + w), (x_5, y_5) = (s, -w) where $-x_2 = -x_3 = s_1$, $x_4 = x_5 = s_2$, $y_2 = -y_3 = w_1$ and $y_4 = -y_5 = w_2$. Then

$$F(\theta) = 1-4\sigma+2e^{iks_1\cos\theta}\cos(kw_1\sin\theta) + 2e^{iks_2\cos\theta}\cos(kw_2\sin\theta) \quad (15)$$

The magnitude squared is:

$$G(\theta) = (1-4\sigma)^2 + 4\sigma(1-4\sigma)\cos(ks_1\cos\theta)\cos(kw_1\sin\theta) + 4\sigma^2\cos^2(kw_1\sin\theta) + 4\sigma(1-4\sigma)\cos(ks_2\cos\theta)\cos(kw_2\sin\theta) + 4\sigma^2\cos^2(kw_2\sin\theta) \quad (16)$$

With the function $G(\theta)$, there are several possibilities for minimising the most significant angle range by determining precisely each outrigger displacement, σ, the stagger, s, and the clearance factors, w.

3. CFD RANS Solver

This study used commercial ANSYS 15.0 CFD

software according to ITTC guidelines (2011). ICEM-CFD generated the meshing and domain of the model in a repetitive procedure. Moreover, CFX-CFD was used to analyse resistance and their components. The domain boundary of the inlet (Fig. 1) was set at 1 Lpp (Length of perpendicular) from the bow, while the outlet was 2 Lpp from the stern. The side was positioned at 1 Lpp from the plane of symmetry, while the bottom 1 Lpp from the keel and the top 0.5 Lpp from the keel.

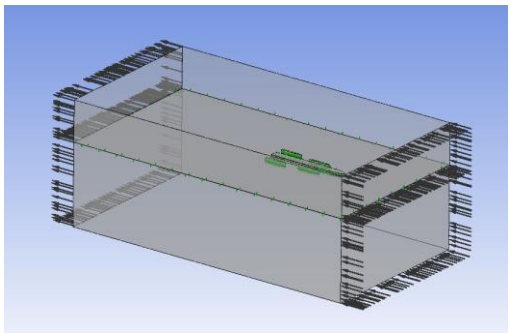

Fig. 1. CFD domain of warp–chine pentamaran.

The converged number of meshing elements and a numerical uncertainty assessment were taken to verify the analytical result of resistance. Meshing with unstructured elements has applied to a mix of prismatic and tetrahedral cells. The mesh processing was repeated seven times to estimate errors and uncertainties. Element sizes for both boundary and ship hulls were varied, i.e., 0.1; 0.005 to 0.002. Convergence was achievable when the force values are not significant for some changes in the number of meshing elements. It obtained for element's size of 0.022 and the model element's size in 0.002. The total number of elements and size of the mesh was taking into account the value of Y^+ in the meshing process. The initial mesh created 8.5 million elements, then increased to 19.9 million, as exhibited in Fig. 2.

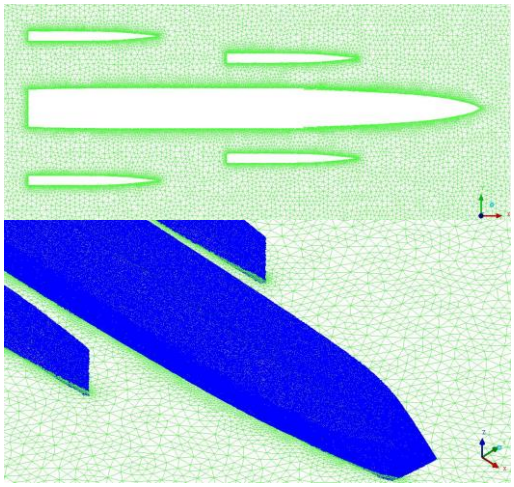

Fig. 2. Mesh element of warp–chine pentamaran.

The volume fraction in multiphase flow is considered to preclude a large residual. Average residuals assumed by repeated convergence through the residual *Root Mean Square* (*RMS*) of a domain required in 10-4. Simulations took the *Shear Stress Transport* (SST), which was a turbulence model commonly used in hydrodynamic analyses of ships. SST consisted of a variety of turbulence models, that in the inner boundary layer as k-ω model, and the outer boundary layer as well as the free stream as k-ε model (Ferziger & Peric, 2002).

4. THE CONTEXT OF WARP–CHINE RESEARCH

Several previous studies have indicated that the chine hull form has several advantages as opposed to other hulls. Chengyi (1994) experiments on catamarans with the chine hull form showed that the reduction in wave resistance and interference tended to decrease at Fn > 0.5. Blount (1995) compared the chine and NPL (National Physical Laboratory) hull form, finding that chine was favourable at Fn > 0.75, although not in its seakeeping performance. Moraes *et al*. (2004) studied catamarans with the chined hull and the Wigley hull. They establish the wave resistance of the chined hull tends to decrease at high speeds compared to the Wigley hull. Begovic and Bertorello (2012) found that a chine hull with a deadrise angle of 25º provided better performance in storm conditions. According to Bari *et al*. (2016), the deadrise angle of 20º increased the Fn, the lift coefficient and the small clearance of the outriggers. In general, this form has advantages such as reducing resistance, greater ease and faster construction process. The studies on optimising the warp–chine were conducted by Savitsky *et al*. (2007), Ghassemi and Gilik (2008) and Taunton *et al*. (2011). The optimal research of chine on Multihull was conducted by Begovic *et al*. (2004), Brizzolara *et al*. (2005) and Dubrovsky (2004).

4.1 Pentamaran Characteristics

The warp–chine pentamaran of this work consists of the main hull with a deadrise angle of 20º and four side-hulls of 35º. A hard chine of the main hull is recommended by Savitsky and Koebel (1993) as a proper hull in achieving minimum resistance. And four of side hulls with an ordinary V form. Pentamaran's midship view in Fig. 3, as an arrow trimaran formation is presented in Fig. 5. Furthermore, Table 1 is describing the dimensions of pentamaran. For this design, warp–chines models with a constant draft in the ratio dimension the length/beam of the main hull, L/B=11.333, and the beam/draught ratio, B/T=5.279. The length/beam ratio of outriggers, L/B=13.8, and the beam/draught ratio, B/T=2.5.

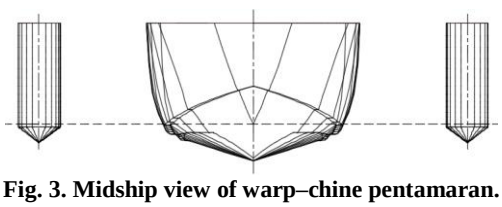

Fig. 3. Midship view of warp–chine pentamaran.

Table 1 Principal dimensions of the model

Dimension	Main hull	Outrigger
WL length (mm)	1435.9	414
Beam on WL (mm)	126.7	30
Draft (mm)	24	12
Height (mm)	90	78
Wetted area (mm^2)	17.68×10^4	14.87×10^3
Vol. displacement (mm^3)	20.45×10^5	69.01×10^3
Displacement (Kg)	2.0378	0.0688
Deadrise (degree)	20	35
Length: Beam ratio	11.333	13.801
Beam: Draft ratio	5.279	2.5
Total Displacement (Kg)	2.313	

4.2 Pentamaran Optimisation

Several Multihull studies have shown that minimum wave resistance is generated at only several speeds. Tuck and Lazaukas (1998) obtained a pentamaran with the optimal minimisation of wave-making in which the main hull had a 3/8 of the total displacement. While each intermediate side hull had a 1/4, and each outer side hull had a 1/16. Even they founded the optimal configuration occurring on the side hull is adjacent with an impractical arrangement. Initial studies on warp-chine pentamaran had been carried out to find the interval constraint of the lateral and longitudinal position of pentamaran side-hulls (Sulistyawati *et al*. 2019a, b). The main hull of the pentamaran model had a 7/8 of the total displacement, and a total of four outriggers had a 1/8. The study revealed the effective reduction of wave resistance between ranges 0.36L and 0.42L, with a clearance of both at 1.05 Bml for the forward outriggers (Cl_1) and 1.5 Bml for the after outriggers (Cl_2), as shown on models B and D.

This work is extended to optimise the configuration of warp–chine pentamaran. Configuration optimisation was achieving optimal through wave cancellation from the ship's performance system based on the maximum wave height generated, wave-making and the total resistance. The pentamaran was optimised by a computer "Godzilla" program with genetic algorithm techniques aimed at minimising the total resistance. At fixed displacement, σ, by varying the stagger, s, and the clearance, w, to reduce the interference factor function $G(\theta)$ in Eq. (16).

The optimisation process with design optimisation procedures, such as in the flow diagram shown in Fig. 4. Godzilla optimisations over a range of design speeds in an integer between 1 and 50 inclusive. The speed range used in this process is 1.54, 1.92 and 2.30 (m/s), then 2.69, 3.07, 3.46 and 3.84 (m/s) corresponding to Fn 0.4-1.0. Detail configurations of all models are identified in Table 2. The "L" in stagger (S_T) referred to the total ship length, while "Bml" in clearance (Cl) referred to the width of the main hull.

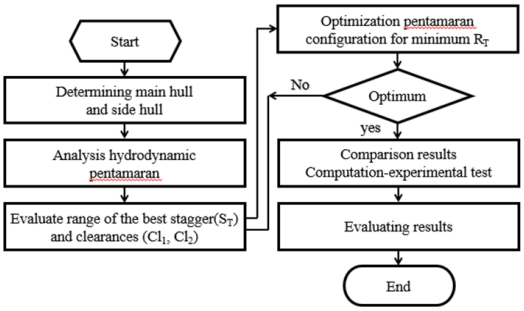

Fig. 4. Pentamaran optimisation procedures.

Table 2 Model configurations

Model	Stagger (m)	Clearance-1 (m)	Clearance-2 (m)
B	0.36L	1.05Bml	1.50Bml
D	0.42L	1.05Bml	1.50Bml
Opt	0.36L	1.35Bml	1.50Bml

The optimisation results obtained the optimal model (Fig. 5) had stagger 0.36L with a clearance of 1.35Bml for the forward outriggers and 1.5Bml for the after outriggers. As a proper configuration of cancelling wave, and achieving minimal resistance.

4.3 Test Set-Up

The tests were conducted in the towing tank of Institut Teknologi Sepuluh Nopembers (ITS) Indonesia, which had the following dimensions: 50 m long, 3 m wide and 2 m deep. Three cameras were mounted on the front between the hull and at some distance from the stern (Fig. 6).

The configuration of the model achieved the optimal results for minimum total resistance is exhibited in Fig. 5. The test setup is shown in Fig. 6. The separation or clearance (Cl_1, Cl_2) and the longitudinal or stagger (S_T) are indicated in meters. The test ranged from Fn 0.1–0.65, which corresponded to speeds of 0.58–2.30 m/s. The low-speed test was applied to determine the form factor (k+1) of the model based on the Prohaska method. The wave investigations and resistance started at above Fn 0.35, where the influence of the waves begins to rise. The determination of the wave resistance is approximated by subtracting a friction element in total resistance from the test results. The formulation of wave resistance is in the Neumann–Michell (NM) theory and the ITTC 1957 model ship correlation line, in which the total resistance coefficient C_T is defined as

$$C_T = R_T \Big/ 0.5\rho V^2 S = C_F + C_R = C_V + C_W \qquad (17)$$

Where R_T is the total resistance, C_F is a nondimensional friction coefficient, C_R is a nondimensional residual coefficient. The nondimensional viscous coefficient, C_V, and a nondimensional wave resistance coefficient, C_W, determined by the equation of total resistance R_T, based on the sum of viscous resistance R_V and or frictional resistance R_F in the following equation

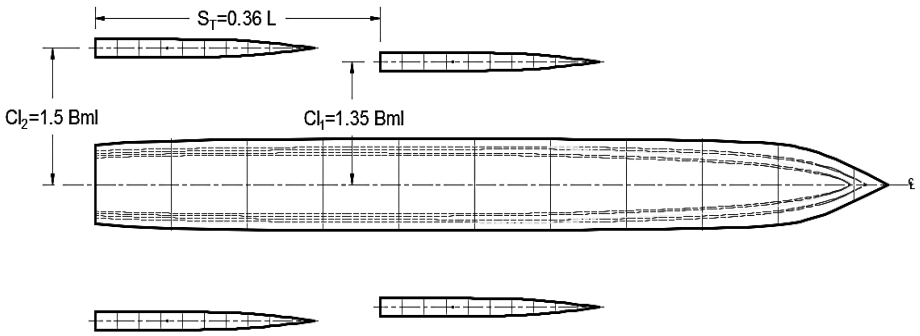

Fig. 5. Optimal configuration (Opt) of arrow pentamaran.

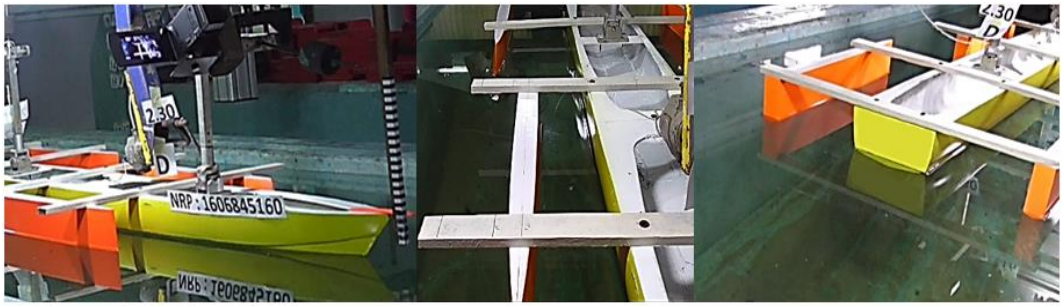

Fig. 6. Pentamaran set-up (captured by three mounted cameras).

$$R_W = R_T - R_V = R_T - (1+k)R_F \tag{18}$$

Where *(1 + k)* is the form factor of the ship's hull that calculated by the Prohaska method. And then, C_F and C_W are defined as:

$$C_F = 0.075 \Big/ (\log_{10} Rn - 2)^2 \tag{19}$$

$$C_W = R_W \Big/ 0.5\rho V^2 S \tag{20}$$

4.4. Uncertainty Analysis

The uncertainty analysis was based on the towing test data according to ITTC's 2002 regulations in a single test. The uncertainty of the total resistance coefficient test U_{CT} according to

$$(U_{CT})^2 = (B_{CT})^2 + (P_{CT})^2 \tag{21}$$

where B_{CT} is bias limit, and P_{CT} is a precision limit, which calculated as

$$(B_{CT})^2 = (\frac{\partial C_T}{\partial S} B_S)^2 + (\frac{\partial C_T}{\partial V} B_V)^2 + (\frac{\partial C_T}{\partial Rx} B_{Rx})^2 + (\frac{\partial C_T}{\partial \rho} B\rho)^2 \tag{22}$$

$$P_{CT} = K.SDev_{\overline{CT}} \tag{23}$$

Bs is the uncertainty of wetted surface, B_V is velocity uncertainty, B_{RX} is the total bias limit in resistance and $B\rho$ is bias density. The precision limit P_{CT} according to the confidence level K (taken as 2) and standard deviation S_{Dev}. The partial derivatives were calculated using input values of total resistance R_T, gravity g, water density ρ, ship speed V, and water surface area S as follows:

$$\frac{\partial C_T}{\partial S} = \frac{R_x}{0.5\rho V^2}\left(-\frac{1}{S^2}\right) \tag{24}$$

$$\frac{\partial C_T}{\partial V} = \frac{R_X}{0.5\rho S}\left(-\frac{2}{V^3}\right) \tag{25}$$

$$\frac{\partial C_T}{\partial R_x} = \frac{1}{0.5\rho V^2 S} \tag{26}$$

$$\frac{\partial C_T}{\partial \rho} = \frac{R_X}{0.5V^2 S}\left(-\frac{1}{\rho^2}\right) \tag{27}$$

Based on the model dimension (Table 1), the assumed error was in the hull form of 0.0001 m. An increase in model weight of 0.035 kg gives, with ρ=1000 kg/m3 and a water plane area in total of 0.236 m2, an additional draught with error in displacement ±0.035 is 0.035/0.024= 0.0014583 mm. With a total waterline length (2xLength of water line, *Lwl*) of 2.8718 m, this results in an increased wetted surface of 0.0014583 x 2.8718 = 0.00000418804 m^2 per kg.

For the deviation in the displacement of ±0.0525 kg, the error in weight displacement equals 0.0735/4.626 = 0.01588846 %, the error in draught equals 0.00010719 mm, and the error in the wetted surface equals 0.0000003078 m. The test obtained the error in the wetted surface 1.000474×10^{-4} m corresponding to 0.01 % of the nominal total wetted surface area of 0.2361 m.

The summary of the standard uncertainty test for model B, D and the optimal model (Opt) estimates in Table 3–5.

Table 3 Total resistance coefficient uncertainty of model B (S_T 0.36L; Cl_1 1.05Bml; Cl_2 1.5Bml)

m/s	C_T	$(\partial C_T/\partial S)$ $*B_S$	$(\partial C_T/\partial V)$ $*B_V$	$(\partial C_T/\partial Rx)$ $*B_{Rx}$	$(\partial C_T/\partial \rho)$ $*B_\rho$	B_{CT}	P_{CT}	U_{CT}	$\pm C_T$ error
1.502	6.68	8.01E-12	1.03E-09	3.37E-07	2.03E-11	0.000582	0.00022	0.000623	0.623
1.663	6.29	7.10E-12	9.15E-10	2.26E-07	1.80E-11	0.000477	0.00018	0.000509	0.509
1.824	5.99	6.44E-12	8.30E-10	1.58E-07	1.63E-11	0.000398	0.00013	0.000420	0.420
1.985	5.64	5.71E-12	7.36E-10	1.14E-07	1.45E-11	0.000338	0.00011	0.000355	0.355
2.146	5.28	5.00E-12	6.45E-10	8.42E-08	1.27E-11	0.000291	0.00008	0.000302	0.302
2.307	4.84	4.20E-12	5.42E-10	6.35E-08	1.07E-11	0.000253	0.00006	0.000261	0.261
2.468	4.50	3.63E-12	4.68E-10	4.89E-08	9.23E-12	0.000222	0.00005	0.000227	0.227

Table 4 Total resistance coefficient uncertainty of model D (S_T 0.42L; Cl_1 1.05Bml; Cl_2 1.5Bml)

m/s	C_T	$(\partial C_T/\partial S)$ $*B_S$	$(\partial C_T/\partial V)$ $*B_V$	$(\partial C_T/\partial Rx)$ $*B_{Rx}$	$(\partial C_T/\partial \rho)$ $*B_\rho$	B_{CT}	P_{CT}	U_{CT}	$\pm C_T$ error
1.502	6.71	8.08E-12	1.04E-09	3.37E-07	2.05E-11	0.000582	0.00021	0.000617	0.617
1.663	5.93	6.31E-12	8.13E-10	2.25E-07	1.60E-11	0.000476	0.00016	0.000503	0.503
1.824	5.73	5.89E-12	7.59E-10	1.57E-07	1.50E-11	0.000398	0.00012	0.000416	0.416
1.985	5.52	5.47E-12	7.05E-10	1.14E-07	1.39E-11	0.000338	0.00010	0.000352	0.352
2.146	5.16	4.78E-12	6.16E-10	8.40E-08	1.21E-11	0.000291	0.00007	0.000300	0.300
2.307	4.79	4.12E-12	5.31E-10	6.34E-08	1.05E-11	0.000253	0.00006	0.000260	0.260
2.468	4.42	3.50E-12	4.52E-10	4.88E-08	8.90E-12	0.000222	0.00004	0.000226	0.226

Table 5 Total resistance coefficient uncertainty of model Opt. (S_T 0.36L; Cl_1 1.35Bml; Cl_2 1.5Bml)

m/s	C_T	$(\partial C_T/\partial S)$ $*B_S$	$(\partial C_T/\partial V)$ $*B_V$	$(\partial C_T/\partial Rx)$ $*B_{Rx}$	$(\partial C_T/\partial \rho)$ $*B_\rho$	B_{CT}	P_{CT}	U_{CT}	$\pm C_T$ error
1.502	6.45	7.46E-12	9.62E-10	3.37E-07	1.90E-11	0.000581	0.00021	0.000618	0.618
1.663	5.88	6.20E-12	8.00E-10	2.25E-07	1.58E-11	0.000475	0.00017	0.000504	0.504
1.824	5.64	5.71E-12	7.36E-10	1.57E-07	1.45E-11	0.000397	0.00013	0.000417	0.417
1.985	5.38	5.19E-12	6.69E-10	1.13E-07	1.32E-11	0.000337	0.00010	0.000352	0.352
2.146	5.11	4.68E-12	6.04E-10	8.39E-08	1.19E-11	0.000291	0.00008	0.000300	0.300
2.307	4.82	4.17E-12	5.37E-10	6.35E-08	1.06E-11	0.000253	0.00006	0.000260	0.260
2.468	4.54	3.70E-12	4.77E-10	4.90E-08	9.39E-12	0.000222	0.00005	0.000227	0.227

5. RESULTS AND ANALYSIS

At the optimisation procedure (Fig. 4), the hull determination process and the hydrodynamic analysis had earlier carried out and discussed before the optimisation topic in this paper. Where the investigations were carried out on six configurations of the warp–chine pentamaran model. The results of the comparison of the towing tank test and the computer "Michlet" predictions resulted in the best position of the stagger's range and clearance. The range with the best configuration in reducing total resistance was at stagger (S_T) 0.36L–0.42L. The first clearance (Cl_1) ranged from 1.05Bml–1.5Bml and the second clearance (Cl_2) at the position of 1.5Bml. The process of optimisation was using the computer "Godzilla" program that took two hours to evaluate a population of 9 million. As explained in subsection 4.2, the optimisation process produced the optimal model with the objective function of minimum total resistance, as shown in Fig. 5: stagger (S_T) of 0.36L, the first clearance (Cl_1) of 1.35Bml and the second clearance (Cl_2) of 1.5Bml.

Figures (7)–(9) show comparisons of the test measurement in the towing tank and the calculation of Michell-based tools and CFD on wave coefficients C_W, and the total resistance coefficients R_T. The configurations of S_T 0.36L; Cl_1 1.05Bml; Cl_2 1.5Bml (Fig. 7) as model B is consistent with the computer calculations and the towing test results of the total resistance coefficient. Nonetheless, the wave resistance coefficient shows a significant deviation. The configurations at S_T 0.42L, Cl_1 1.05Bml, Cl_2 1.5Bml (Fig. 8) as model D also indicates that the computer calculations of the total resistance coefficients provide fairly reasonable accuracy, but not for the wave resistance coefficients. While for the configurations at S_T 0.36L, Cl_1 1.35Bml, Cl_2 1.5B ml (Fig. 9) as the optimal model is consistent between the computer calculations and the measurement of the test regarding the total resistance coefficient and wave resistance coefficient. Comparison of CFD computing with the test measurements on models B and D have a significant deviation in the total resistance coefficient and shows consistency in the wave coefficient. Meanwhile, on the optimal model (Opt), results of CFD on both wave coefficient and total resistance appeared to disagree from the experiment mostly.

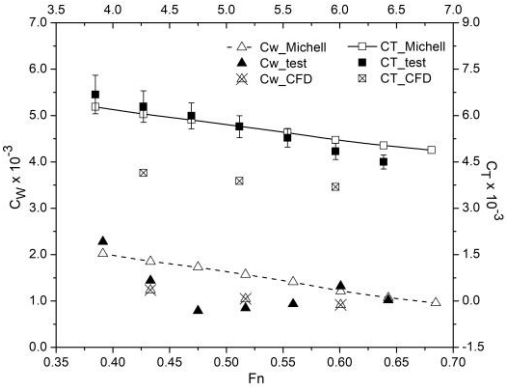

Fig. 7. Comparison of C_W and C_T on B (S_T 0.36L; Cl_1 1.05Bml; Cl_2 1.5Bml).

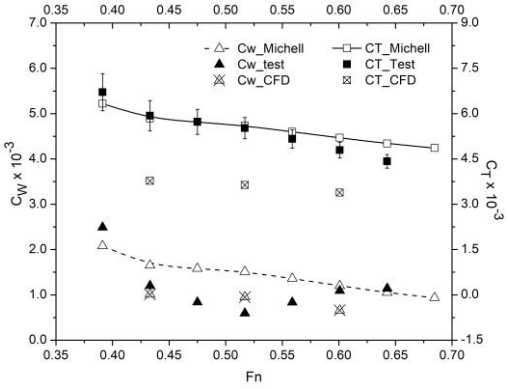

Fig. 8. Comparison of C_W and C_T on D (S_T 0.42L; Cl_1 1.05Bml; Cl_2 1.5Bml).

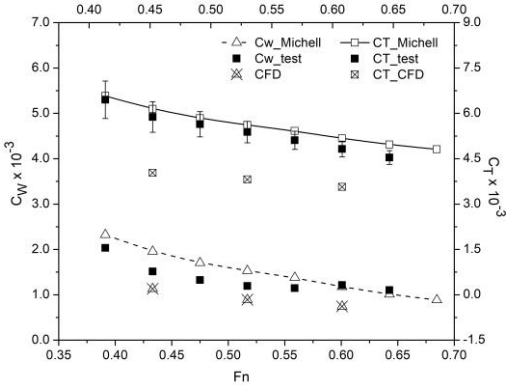

Fig. 9. Comparison of C_W and C_T on Opt. (S_T 0.36L; Cl_1 1.35Bml; Cl_2 1.5Bml).

Then on Fig. 10 presents results for the frictional resistance coefficient C_F and the residual resistance coefficient C_R. The frictional resistance C_F was acting on a hull form for Michell calculation, and the test measurement refers to Eq. 19, while for CFD could be calculated in CFX-Post by performing count in an area integral of the wall shear in the *x*-direction.

Michell's calculation results and the test measurements of the total resistance coefficient C_T show a consistent trend, especially at Fn ≥ 0.4. The average deviation of C_T between the results of the Michell–based tool and the test measurements are obtained by model B about 6.85%, model D of 8.70% and the optimal model (Opt) of 2.953%. Regarding the wave resistance coefficients C_W, all configurations show considerable deviations, especially between Fn 0.4–0.5. The average deviation model B of 0.44%, model D of 1.26% and Opt of 9.049%.

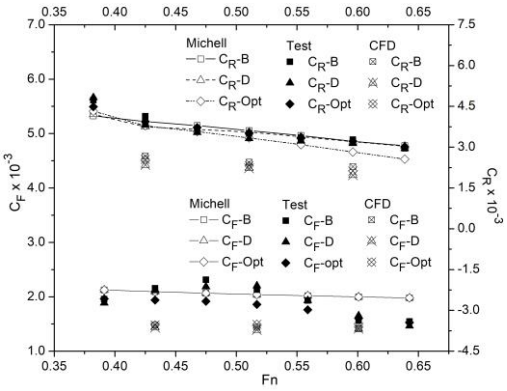

Fig. 10. Comparison of C_F and C_R.

While CFD calculations and the test measurements have a most significant deviation with average differences of C_T for each model are 23.98% (B), 23.59% (D) and 29.16% (Opt.), while in terms of C_W are 4.09% (B), 5.24% (D) and 29.82% (Opt). The frictional resistance coefficient C_F at Fig. 10 shows that the results of Michell-based tools of all of the models have a coinciding trend with the test, while CFD produces many differences. For the residual resistance coefficient C_R, provides an appropriate graphic pattern with wave resistance coefficient.

The initial results of the configuration range and the optimal model on the wave resistance coefficients and total resistance coefficients were evaluated in speeds ranges Fn 0.35–0.65. The comparison results of the towing test, Michell's and CFD computation on the wave and the total resistance coefficients of three configurations are plotted in Figs. (11)–(12), respectively. The towing test results of the lowest range (B) to the highest (D) of the wave and total resistance coefficients show a decrease of 6.386% and 2.332%, respectively. The test results of model B to Opt (the optimal model) also show a reduction of the wave and the total resistance coefficients of 9.385% and 3.569%, respectively. Nonetheless, the difference value of the total resistance test for all models shows the estimated error (uncertainty) in the same range (see Table 3–5).

As for Michell's calculation, the result comparison of model B and model D for C_W and C_T show decreases of 3.942% and 0.903%, respectively. Whereas model B to the optimal model (Opt) also indicates a reduction of 1.23% for C_W and 0.311% for C_T. Meanwhile, the CFD results from models B to D has a decrease of 18.59% for C_W and 8.04% for C_T. And from model B to Opt also has a reduction of 13.43 % for C_W and 2.58% for C_T.

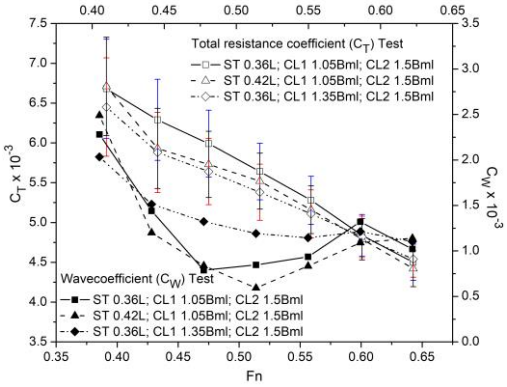

Fig. 11. Test comparison of C_W and C_T.

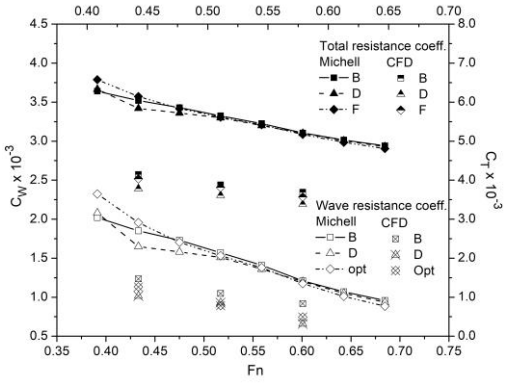

Fig. 12. Computation on C_T and C_W.

This work also analyses on transverse, diverging and interference waves by the Michell-based tool. Figure 13 represents the results of the three configurations of the transverse wave coefficients (C_W-*trans*) and the diverging wave coefficients (C_W-*div*). The trend of all models on the transverse wave (C_W-*trans*) tends to increase at below Fn 0.5 with the highest point at Fn 0.475 and then gradually decrease. The hump of the diverging wave (C_W-*div*) occur at Fn 0.4 and then gradually decrease. The highest C_W-*trans* are obtained by model B (S_T 0.36L; Cl_1 1.05Bml; Cl_2 1.5Bml) and then the optimal model (S_T 0.36L; Cl_1 1.35Bml; Cl_2 1.5Bml) and subsequently model D (S_T 0.42L; Cl_1 1.05Bml; Cl_2 1.5Bml). At Fn above 0.5, model B is getting the highest C_W-*div*, then model D and subsequently the optimal model. The interference wave coefficient (C_W-*int*) in Fig. 14, at below Fn 0.5, model B has the best interference indicate by a negative value. However, after Fn 0.5, the optimal model has the lowest interference value compare with the others. The negative value of interference is representing the smaller wave resistance of Multihull than the total wave of each hull in the wave system. As increasing Fn, interference of the optimal model trend tended to show a larger decrease than the others did.

6. DISCUSSION

The proper selection and evaluation of stagger *s*, and clearance *w*, in Eq. (16) to minimise the objective function and yielded the optimal configuration. That was producing a minimum total resistance without changing the hull shape and the displacement of pentamaran. Some deviations in the calculation of the resistance components in the computer "Michlet" program and the test measurements of six configurations had been discussed and evaluated by Sulistyawati *et al*. (2019 a, b). The accuracy of the wave resistance was based on the calculation of viscous resistance, as described in Eq. (18). Difficulties in determining the form factor (1+k) affected the exact magnitude of the viscosity, so the value of the wave resistance obtained provided a considerable deviation. The analysis of the test results was getting the difference in form factors (1+k): 2.250 (B), 2.237 (D) and 2.251 (Opt). While on Michell's based-tool was obtained: 2.0 (B), 1996 (D) and 2.0 (Opt). CFD were obtained: 1.97 (B), 1.93 (D) and 1.955 (Opt).

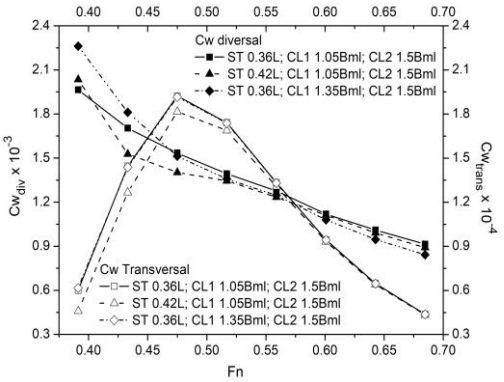

Fig. 13. Michell-based tool on transversal and divergent wave.

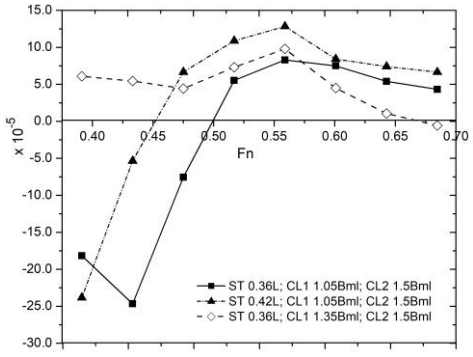

Fig. 14. Michell-based tool on C_W-interference.

Figures (7)–(9) show the conformity of the results of Michell's based tool and the results of the towing test, especially at Fn ≥ 0.4. However, a weak comparison between CFD and the test measurements. Initial estimates of the possible effects of trim and sinkage to the significant differences in the resistance measurement with the calculation of both Michell's based tool and CFD, apparently do not have enough evidence. The calm water testing showed little changing on the trim and sinkage, which proved on B_{RX} to be a component of the effect of trim and sinkage, giving a small presentation value (max. 0.089% of R_T). Regardless of errors and uncertainties encountered in this

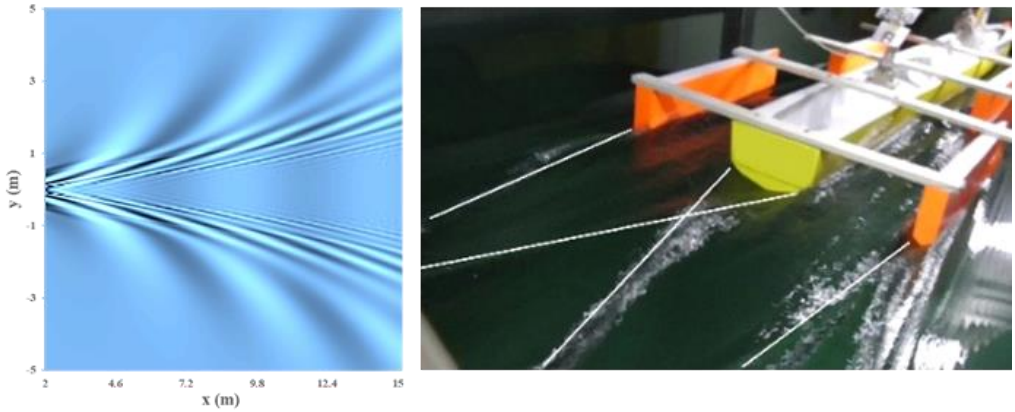

Fig. 15. Captured far-field wave pattern of model B by Michell based-tool (left) and during the test at 60-second (right) at Fn = 0.6.

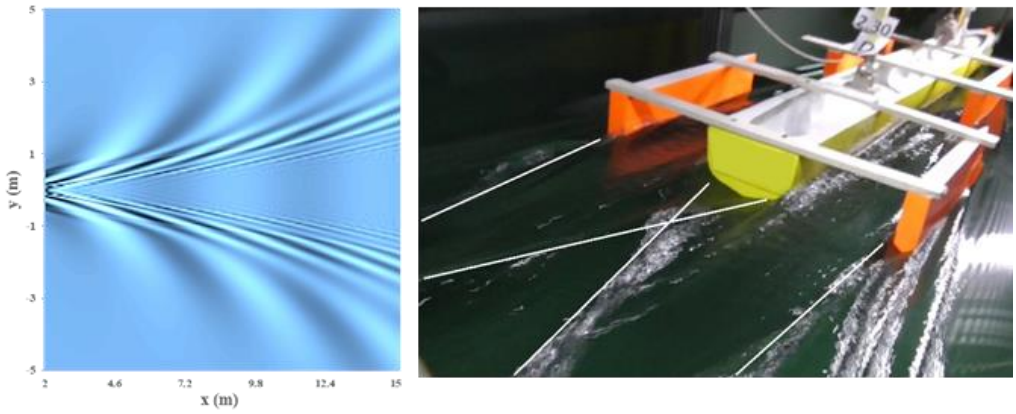

Fig. 16. Captured far-field wave pattern of model D by Michell based-tool (left) and during the test at 60-second (right) at Fn = 0.6.

study, a comparison between CFD, Michell's based tool and experiment had been conducted by Tuck and Lazaukas (2008) on the total resistance of a ship. They obtained an over-estimation of Michell's results at about 10% than the test, while CFD with fine grid at much lower estimates.

The resistance reduction was generated by the boundary layer and the wake from appropriating the hull shape and proper placement of the outriggers. The complexity of the interference factor and transversal-divergent wave from the configuration was in such a way that it delivered destructive waves in hull-to-hull interaction. These waves eliminated each other, thereby reducing the wave resistance, then directly decreasing the total resistance. The optimal model (S_T 0.36L; Cl_1 1.35Bml; Cl_2 1.5Bml) as shown in Figs. 13–14 has good cancellation of the transversal wave and lower wave interference. So, it directly generates a large number of total resistance reductions, especially at above Fn 0.5, although it produced higher wave resistance than the two others. The low deviation in the results of the towing test and the computer "Godzilla" program, as shown in Figs. 10-12 indicate the ability of this tool in the optimisation process.

Figures (15)-(17) show the comparison of the wave pattern from capturing of the test (left) and Michell's based-tool in the far-field (right). Even though these two devices do not show clear apparent similarities, but thin layers inside the wave pattern envelope of Michell's consistent with the pattern from the test. The layer pattern (wave spectrum) is an illustration of Eq. (9) as a linear superposition of the far-field wave patterns on the sectoral patch in an area at the back of the ship. The dark blue colour indicates the deepest troughs, and the white colour means the highest crests (see the left figure in Figs. (15)-(17). The optimal model (S_T 0.36L; Cl_1 1.35Bml; Cl_2 1.5Bml) produces a more significant wave on the far-field than the two others (see Fig. 17). These figures suggest suitability with the test resistance measurement in Fig. 11. The far-field wave pattern of model B (S_T 0.36L; Cl_1 1.05Bml; Cl_2 1.5 Bml at Fn 0.6) in Fig. 15 had calm flow with a slight ripple. While model D (S_T 0.42; Cl_1 1.05Bml; Cl_2 1.5Bml) as shown in Fig. 16 generated flows with more ripples, but a little better than Opt model. This study did not compare the warp-chine hull with the rounded hull type, but has shown that the warp-chine capable of cancelling waves and decreasing total resistance about 10% of the proper placement of stagger and clearance.

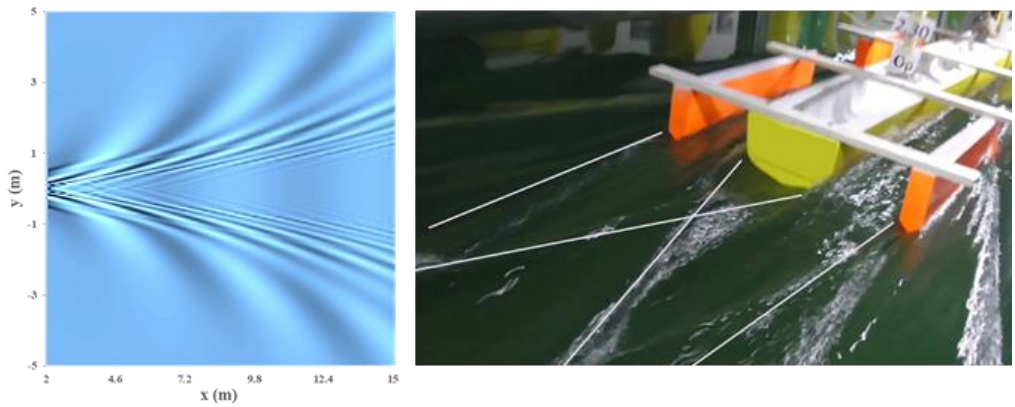

Fig. 17. Captured far-field wave pattern of model Opt by Michell based-tool (left) and during the test at 60-second (right) at Fn = 0.6.

7. CONCLUSION

This study has investigated the hydrodynamic performance and optimised the warp-chine pentamaran in various configurations based on Michell's theory, CFD and validated with the test. Towing tank tests on calm water were conducted in compliance with the ITTC procedures and guidelines. The results show significant deviations between experiments and Michlet calculation, mainly when Fn < 0.4. It arguably occurred due to an inaccuracy in determining the form factor from test measurements at low speeds and estimates on Michell-based tools. Then, substantial differences were observed in CFD, implying a need to refine the mesh model to improve its performance.

The analysis and observations indicated that the objective function with the minimum of the total resistance did not provide the minimum value of other resistance components. The optimal determination in a design configuration did not generate lower resistance components at each speed, depending on certain speed limits. The estimated error (uncertainty) of the total resistance of the optimum configuration was still at an uncertain range of the two others. However, this optimisation has confirmed the results of previous research on the pentamaran warp-chine. These results prove that the stagger range 0.36L-0.42L where the front outriggers and the after outriggers were not in line clearance are high in wave cancellation and resistance reduction. This study also has proven a computer "Godzilla" program (based on Michell's theory) as a simple, efficient, effective and well tool suited to the optimisation of configuration. This tool also compatible with implementing the far-field wave pattern of the warp–chine pentamaran. In future works, Multihull optimisation technique with the multi-objective function will be developed by combining the evaluation of hull shape. Also, on modifications a symmetrical or asymmetrical hull to reduce interference effects between the hulls in near and far-field.

ACKNOWLEDGEMENTS

This research was funded by the Indonesian Scholarship of Indonesian Endowment Fund for Education (LPDP). The authors thank the facility for its support of the towing tank at the Institut Teknologi Sepuluh November (ITS), Surabaya, Indonesia. The authors also thank Dr Leo Lazaukas at the University of Adelaide for the solution of the Godzilla optimisation process.

REFERENCES

Aubault, A., and R. W. Yeung (2012). Interference resistance of multi-hull vessels in finite-depth waters. *Journal of Marine Systems and Ocean Technology* 7 (2), 107-116.

Bari, G. S., and I. M. Konstantin (2016). Hydrodynamic modelling of planning catamarans with symmetric hulls. *Ocean Engineering* 115, 60-66.

Begovic, E., and C. Bertorello (2012). Resistance assessment of warped hull form. *Ocean Engineering* 56, 28–42.

Begovic, E., Bertorello, C., Caldarella and P. Cassella (2004). Pentamaran hull for medium-size fast ferries, In Chang and Yeow's (Eds.), *Hydrodynamics VI: theory and applications*, 23–27.

Blount, D. L. (1995, September). Factors influencing the selection of a hard chine or round-bilge hull for high Froude numbers. In C.F.L. Kruppa (Ed.), *Proceedings of the 3th International Conference on Fast Sea Transportation*, Lubeck-Travemunde, Germany. 1 (3), 18.

Brizzolara, S., D. Bruzzone, and E. Tincani (2005, June). Automatic optimisation of a trimaran hull form configuration. *Proceedings of the 8th International Conference on Fast Sea Transportation*, Saint Petersburg, Russia, 49–56.

Chengyi, W. (1994). Resistance characteristic of high-speed catamaran and its application. *Ship building of China* 3, 28-39.

Day, A. H., and L. J. Doctors (2001). Rapid estimation of near- and far-field wave from ships and application to hull form design and optimization. *Journal of Ship Research* 45, 73–84.

Day, S., D. Clelland, and E. Nixon (2003). Experimental and numerical investigation of arrow trimarans. In P. Casella's (Ed.), *Proceedings of the 7th International Conference of Fast Sea Transportation* 3, Ischia, Italy, pp. 23-36. Naples: Dipartimenta Ingegneria navale, Universt`a di Napoli.

Doctors, L. J., A. H. Day, and S. Node (1995, November). Hydrodynamically optimal hull forms for river ferries. *International Symposium on High-Speed Vessels for Transport and Defence, RINA:* London, England, pp. 15.

Doctors, L. J., and A. H. Day (2000, November). Wave-free river-based air-cushion vehicles. *Proceedings of International Conference on Hydrodynamics of High-speed Craft Wake Wash and Motions Control*, London, England, 12.1–12.9.

Dubrovsky, V.A. (2004). Concept design of outrigger ships. In *RINA International Conference, Design & Operation of Trimaran Ships*, London.

Dudson, E., and S. Harries (2005, June). Hydrodynamic fine-tuning of a pentamaran for high-speed sea transportation services. *Proceedings of the 8th International Conference on Fast Sea Transportation*, St. Petersburg, Russia, pp. 9.

Ferziger, J. H., and M. Perić (2002). *Computational methods for fluid dynamics* 3, 196-200. Springer, Berlin, Germany.

Ghassemi, H., and M. Ghiasi (2008). A combined method for the hydrodynamic characteristics of planning crafts. *Ocean Engineering* 35, 310–322.

Ikeda, Y., E. Nakabayashi, and A. Ito(2005). Concept design of a pentamaran-type fast Ro-Ro ship. *Journal of the Japan Society of Naval Architects and Ocean Engineers* 1, 35-42

ITTC (International Towing Tank Conference). (2011). Recommended Procedures and Guidelines Practical Guidelines for Ship CFD Applications, 7.5-03-02-03.

ITTC (International Towing Tank Conference). (2002). Recommended Procedures and Guidelines Testing and Extrapolation Methods Resistance, Uncertainty Analysis, Example for Resistance Test, 7.5-02-02-02

Lazauskas, L. (1997). Michlet. http://www. cyberiad.net/michlet.htm

Lazauskas, L. (1997). User's guide for GODZILLA. *Applied Mathematics Report L970 I.* The University of Adelaide [in preparation], Australia.

Michell, J. H. (1898). The wave-resistance of a ship. *Philosophical Magazine* 45 (5), 106–123.

Moraes, H. B., J. M. Vasconcellos, and R. G. Latorre (2004). Wave resistance for high-speed catamarans. *Ocean Engineering* 31 (17), 2253–2282.

Newman, J. N. (1977). *Marine hydrodynamics*. Cambridge: MIT Press.

Peng, H. (2001). *Numerical computation of multihull ship resistance and motion*. Doctoral dissertation, Ph. D. thesis, Dalhousie University, Nova Scotia, Canada.

Savitsky, D., and J .G. Koebel (1993). Seakeeping Considerations in design and operation of hard chine planning hulls. *Technical Research Bulletin. R-42*. 124 Jersey City (USA): SNAME.

Savitsky, D., M.F. DeLorme, and D. Raju, (2007). Inclusion of whisker spraydrag in performance prediction method for high-speed planning hulls. *Journal of Marine Technology* 44 (1), 35-56.

Sulistyawati W., Yanuar, and A. S.Pamitran, (2019a) Research on pentamaran by model test and theoretical approach based on Michell's integral. *CFD Letters* 11 (3), 117-128.

Sulistyawati, W., Yanuar, and A. S. Pamitran. (2019b) Warp-chine on pentamaran hydrodynamics considering to reduction in ship power energy. *Energy Procedia* 156, 463-468, Nagoya, Japan.

Tarafder, M. S., M. T. Ali, and M. S. Nizam (2013). Numerical prediction of wave-making resistance of pentamaran in unbounded water using a surface panel method. *Procedia Engineering* 56, 287-296.

Taunton, D.J., D.A. Hudson, and R.A. Shenoi (2011). Characteristics of a series of high-speed hard chine planning hulls. Part II: performance in waves. *International Journal Small Craft Technology* 153, B1–B22.

Tuck, E. O., and L. Lazauskas (2008). *Unconstrained ships of minimum total drag. University of Adelaide*. Applied Mathematics Department, The University of Adelaide.

Tuck, E. O., and L. Lazauskas (1998). Optimum hull spacing of a family of multihulls. *Ship Technology Research Schiffstechnik* 45 (4), 180.

Tuck, E. O., D. C. Scullen, and L. Lazauskas (2001). Ship-wave patterns in The Spirit of Michell. *IUTAM symposium on free surface flows*, 311–318.

Yanuar, Ibadurrahman, K. T. Waskito, S. Karim

and M. Ichsan. (2017). Interference resistance of pentamaran ship model with asymmetric outrigger configurations. *Journal of Marine Science and Application* 16 (1), 42-47.

Yeung, R. W., G. Poupard, and J. O. Toilliez (2004). Interference-resistance prediction and its applications to optimal multihull configuration design. *Transactions of the Society of Naval Architects and Marine Engineers* 112, 142-168.